Int. J. Solids Structures Vol. 23, No. 4, pp. 521–536, 1987
Printed in Great Britain.

0020–7683/87 $3.00 + .00
Pergamon Journals Ltd.

LEAST-WEIGHT DESIGN OF PERFORATED ELASTIC PLATES—I†

G. I. N. ROZVANY,‡ T. G. ONG, W. T. SZETO and R. SANDLER
Department of Civil Engineering, Monash University, Clayton, Victoria, Australia 3168

and

N. OLHOFF§ and M. P. BENDSØE
Department of Solid Mechanics and Mathematical Institute, Technical University of Denmark, DK-2800 Lyngby, Denmark

(*Received* 21 *June* 1985)

Abstract—The paper investigates implications of some recent mathematical developments in the fields of shape optimization and relaxation of variational problems. Considering the least-weight design of perforated elastic plates in either flexure or plane stress for a prescribed compliance, it is shown that at low rib densities microstructures consisting of a combination of first- and second-order infinitesimal ribs is superior to those consisting of purely first-order infinitesimal ribs. Moreover, it is indicated that thin ribs of infinite length/thickness ratio do not contribute significantly to the stiffness in a direction normal to their plane. On the basis of this conclusion, a simple specific cost function is derived and then it is used in the design of circular, uniformly loaded perforated plates with zero value of Poisson's ratio. As a basis for comparison several intuitively selected topographies are optimized for the case of simply supported plates, and in Part II of this study a variational analysis is used to obtain the optimal solutions for plates with simply supported, clamped or loaded edges.

1. INTRODUCTION

This study is concerned with the weight minimization of transversely loaded perforated elastic plates having a constant thickness and a prescribed compliance but a general formulation for plates in plane stress is also discussed.

The present investigation has been prompted by a series of discoveries in plate optimization which have brought about a profound revision of the underlying principles and exposed some unexpected features of least-weight plates. Cheng and Olhoff[1] have found that *stiffener-like formations* appear in elastic plate solutions if the maximum and minimum values of the plate thickness are prescribed and the number of finite elements used are sufficiently large. It was then pointed out by the late Professor W. Prager (Brown University) that the *layout* of such stiffeners is similar to that of *least-weight grillages*, derived independently by both Prager and Rozvany[2, 3]. Subsequent investigations by Olhoff, Cheng, Lurie, Cherkaev and Fedorov[4–6] show that considerably more efficient plate designs can be derived from a *new formulation* in which the set of feasible solutions is extended to functions with an unlimited number of discontinuities. Such designs were obtained numerically via the introduction of a *rib-density function*. A similar concept (beam density) was used implicitly by Prager and Rozvany[2, 3] in deriving least-weight grillages which degenerate into "grillage-like continua" (Prager). For the case of plastically designed plates of a prescribed maximum thickness, Rozvany and co-workers[7, 8] obtained closed-form analytical solutions. The latter study shows that for axisymmetric plates the least-weight solution may contain only two types of regions: (a) solid plate segments with equal principal moments ($M_1 = M_2$) and (b) one-way rib systems of maximum depth. As plate designs with discontinuities in the thickness may not fulfil some assumptions of the classical theory of thin elastic plates, Kohn and Vogelius[9] developed a rigorous model for handling

† The authors wish to acknowledge the late Professor W. Prager's lasting contribution to the methods employed in this project.

‡ Since 1985: FB 10, Essen University, 4300 Essen 1, West Germany.
§ Since 1985: Department of Mechanical Engineering Design, Aalborg University, DK-9220 Aalborg, Denmark.

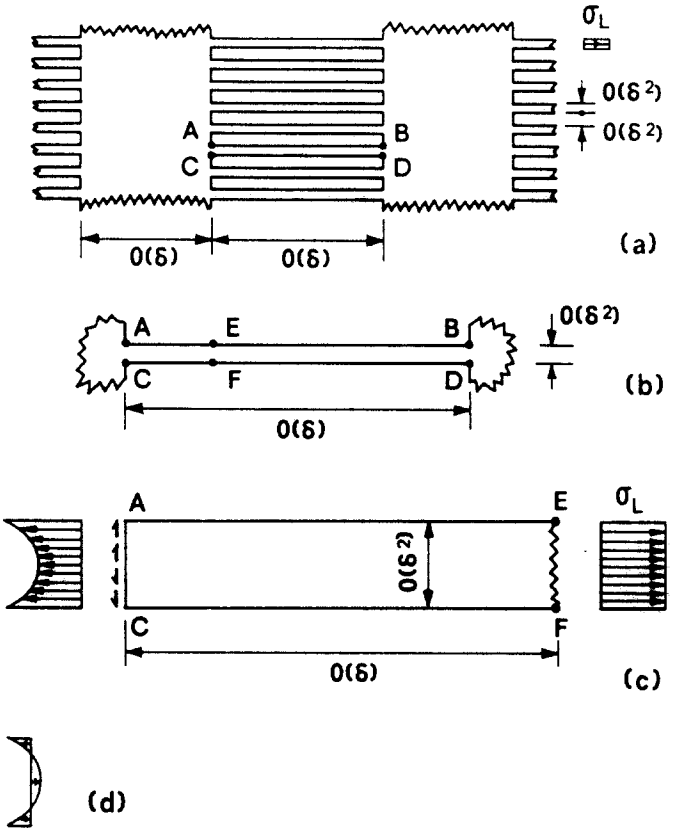

Fig. 1. The correct structural behaviour of a first/second-order microstructure.

rapid changes in the cross-section. Numerical solutions based on solid and ribbed regions were derived for non-axisymmetric boundaries by Bendsøe[10]. Kohn and Strang[11] have also found that in shape optimization problems involving plastic design an infinite number of internal boundaries ("holes") appear in the optimal solution. Mathematical aspects of optimal microstructures for various physical problems involving composites were discussed by Lurie and co-workers[12–16], as well as Kohn and Strang[17, 18].

The above investigations included the study of minimum weight plates consisting of two linearly elastic materials. A common feature of formulations for plates was the underlying assumption that thin ribs can be treated as plate elements so that the effective stiffness of rib-stiffened plates can be obtained by homogenization of the Kirchhoff plate equation. While this line of investigation is of considerable importance, indicating the true nature of the solution for the original mathematical problem, the theoretical optimal solution in some cases may lie outside the range of validity of traditional plate theory or its recent extensions. Also, the optimal solution may be physically unrealistic for other reasons (buckling of ribs, ribs behaving like beams rather than plate elements, etc.). The problems mentioned arise in particular when the elastic modulus (and specific cost) of one material considered tends to zero and thus a composite is replaced by a perforated material (plates containing an unlimited number of "holes"). For these reasons, a formulation based on a physically more realistic microstructure is discussed in this paper.

2. REASONS FOR A NEW MICRO-MODEL

In the papers of Lurie and co-workers[12–16] as well as Kohn and Strang[17], the theoretical optimal solutions for various problems contain regions with two sets of intersecting ribs (layers of material). This type of solution will be confirmed here on the basis of physical arguments for least-weight plane stress and perforated plate problems, i.e. the optimal solutions for such problems will be shown to contain regions with two sets

of intersecting ribs in the principal directions and with spacing of different order. One such set has a first-order infinitesimal spacing (of $O(\delta)$ with $\delta \to 0$) and the other set a second-order infinitesimal spacing (of $O(\delta^2)$, see Fig. 1(a)). Considering a *plane stress* problem first, a typical rib ABCD is shown in Fig. 1(b) and one of its ends in an enlarged version in Fig. 1(c). The considered ends are subjected to (i) some *symmetric* normal stress distribution and (ii) symmetrically distributed shear stresses (since the resultant shear stress is zero in the principal direction and hence the considered rib is also free of in-plane bending). However, the well-known *Saint Venant's principle*[19] states that self-equilibrating load systems acting within an infinitesimal region of an elastic body have no effect on the stresses at a finite (or lower order infinitesimal) distance from such a load. It follows that the shear stresses along AC (Fig. 1(c)) and the non-uniform part of the axial stresses (Fig. 1(d)) do not influence the stresses at a distance of $O(\delta)$ from the end (having a width $O(\delta^2)$) and hence the state of stress along EF (Fig. 1(c)) will consist of uniformly distributed normal stresses in the direction of the rib and vanishing (zero) normal stress in the second principal direction. The shear stress also takes on a zero value along a general cross-section (EF). For a zero value of Poisson's ratio ($\nu = 0$), the lateral strain will also vanish at $O(\delta)$ from the rib ends. In calculating the total compliance $\left(\int_D \sigma_i \varepsilon_i \, dx \, dy \, dz\right)$ for all ribs of $O(\delta^2)$ width, we find therefore that only the longitudinal stresses (σ_L in Figs 1(a) and (c)) have a significant effect because all other stresses spread only over a distance of $O(\delta^2)$ from the rib ends.

Basically the same argument can be extended to *second-order* infinitesimally thin ribs in *perforated plates*. Such ribs have a *first-order* infinitesimal length and a *finite* height (which is small in comparison to the plate span for "thin" plates and could therefore be modelled as a first-order infinitesimal). This implies that the rib thickness is at least one order of magnitude smaller than the height and length of the rib. If such ribs are in the principal directions and body forces are neglected, the ribs will be loaded only along their edges. Again, the edge loads consist of *in-plane* stress resultants and self-equilibrating load systems within infinitesimal regions. Such ribs therefore fulfil all classical assumptions for *in-plane stress problems*[20, pp. 15–34] with significant stress components only parallel to the mid-plane of the ribs. All other stresses, by Saint Venant's principle, may only spread at a distance of $O(\delta^2)$ from the edges and hence their effect on the total compliance can be neglected. The same conclusions will be confirmed by numerical (finite element/finite difference) methods in a subsequent paper.

The above reasoning shows that the treatment of second-order ribs as two-way plate elements in perforated plates might not be entirely realistic from a physical point of view.

3. PROBLEM FORMULATION FOR PERFORATED PLATES

Bearing the above conclusions in mind, we can now formulate our problem as follows. Minimize the total structural weight of a linearly elastic stressed system whose middle surface D is contained in a horizontal plane referred to coordinates (x, y). The considered structure is subjected to vertical loads $p(x, y)$ and its depth at any point can take on only one of two values: (i) zero, or (ii) a given constant h. From areas of zero thickness the load $p(x, y)$ is transmitted by some secondary system whose volume tends to zero and is therefore neglected. It is assumed that the vertical deflections $w(x, y)$ and depth "h" are small in comparison to the horizontal dimensions of D and hence shear and normal (membrane) forces can be neglected in calculating deflections and compliance. As the depth is small relative to the spans, it is further assumed that all normal stresses in the horizontal directions are proportional to the distance from the mid-plane of the plate. Here, only elastic materials having a Poisson's ratio of zero will be considered. On the basis of optimal microstructures derived by Lurie and co-workers[12–16] and Kohn and Strang[17, 18] only the following types of admissible regions are considered in the solution.

(a) A solid plate of depth "h" (which may include "ribs" of finite width).

(b) Regions consisting of systems of "ribs" of infinitesimal width and infinitesimal spacing. The ribs may run in one or several directions and their spacing may be a first- or higher-order infinitesimal.

It can be shown easily through physical reasoning that in any type "b" region above the ribs must run in the "principal" directions. By definition, the torsional moment takes on a non-zero value for any non-principal direction. Considering ribs of depth $h = O(\delta^0)$ and width δ with $\delta \to 0$, the flexural stiffness is $E\delta h^3/12 = O(\delta)$. It follows from the membrane analogy of elastic torsion problems for prismatic bars[20, pp. 303–307] that the *stress function* for such ribs is $O(\delta^2)$ and thus its integral for a cross-section of width δ (representing the torsional stiffness) becomes $O(\delta^3)$. As the torsional stiffness of ribs of infinitesimal width is two orders of magnitude smaller than their flexural stiffness, any non-zero torsional moment over a finite area would produce two orders of magnitude higher compliance than ribs in flexure only, which clearly cannot be optimal. It follows that infinitesimal ribs in the considered optimal solution can only run in the principal directions, which are known to be at right angles.

4. PHYSICAL REASONS FOR THE OPTIMALITY OF MICROSTRUCTURES WITH FIRST- AND SECOND-ORDER RIB SYSTEMS (PERFORATED PLATES IN BENDING OR PLANE STRESS)

In this section, physical reasons based on fundamental principles of elasticity are given for the improved economy of first/second-order rib systems over first/first-order systems. Perforated plates in both plane stress and bending will be considered.

Figure 2(a) shows a modified version of a first/first-order system in which (i) for simplicity, the spacing of the ribs is unity (instead of a first-order infinitesimal), and (ii) the stiffness is the same in both principal directions (in Fig. 2(a) the rib width is "b" for both rib systems). On the basis of the discussion in Section 2 (using Saint Venant's principle), significant two-way stresses occur only over a limited region at the intersections (see shaded area in Fig. 2(a) and some fictitious lines of principal stresses in Fig. 2(b)). Considering the stresses in the ribs in the y-direction, e.g. the extent of stress diffusion over the rib intersection can be represented by some *equivalent width* of cb over a length b of the y-ribs. The value of the *stress diffusion factor* c is chosen in such a way that a uniformly stressed prismatic member along the intersection gives the same stiffness as the real intersection. The actual value of c is being evaluated for various values of b by a detailed numerical analysis and will be discussed in a later paper. However, preliminary indications are that c is greater than 1 and significantly smaller than 2

$$1 < c < 2. \tag{1}$$

Figure 2(c) indicates a first/second-order system in which the rib density $b_1/a_1 = b$ of the second-order system is the same as that of the first/first-order system $b_1 \to 0$ and $a_1 \to 0$. The total material volume of both microstructures is therefore the same. Referring again to the discussion in Section 2, we can see from Fig. 2(d) that the effective width of the first-order ribs in the x-direction will be "b" because the diffusion of the x-stresses into the second-order ribs is restricted to an additional width of $O(\delta)$ with $\delta \to 0$. On the other hand, it follows from Saint Venant's principle again that the stresses transmitted from the second-order y-ribs onto the first-order x-ribs will diffuse into a uniform y-stress within a distance of $O(\delta)$ from the edge of the x-ribs of width b (see Fig. 2(d)). This means that *the entire volume of the x-ribs can be assumed to be uniformly stressed in two directions* since the zone of stress diffusion is negligibly small, i.e. $O(\delta)$.

Next, we shall determine the mean stiffness $S_{AV} = (S_x + S_y)/2$ for the two systems in Fig. 2. The discussion that follows is restricted to relatively low density microstructures with $b \ll 1$ and a zero value for the Poisson's ratio ($\nu = 0$). Considering the *flexural system* in Fig. 2(a), the principal moments (per unit width) in the x- and y-directions will be

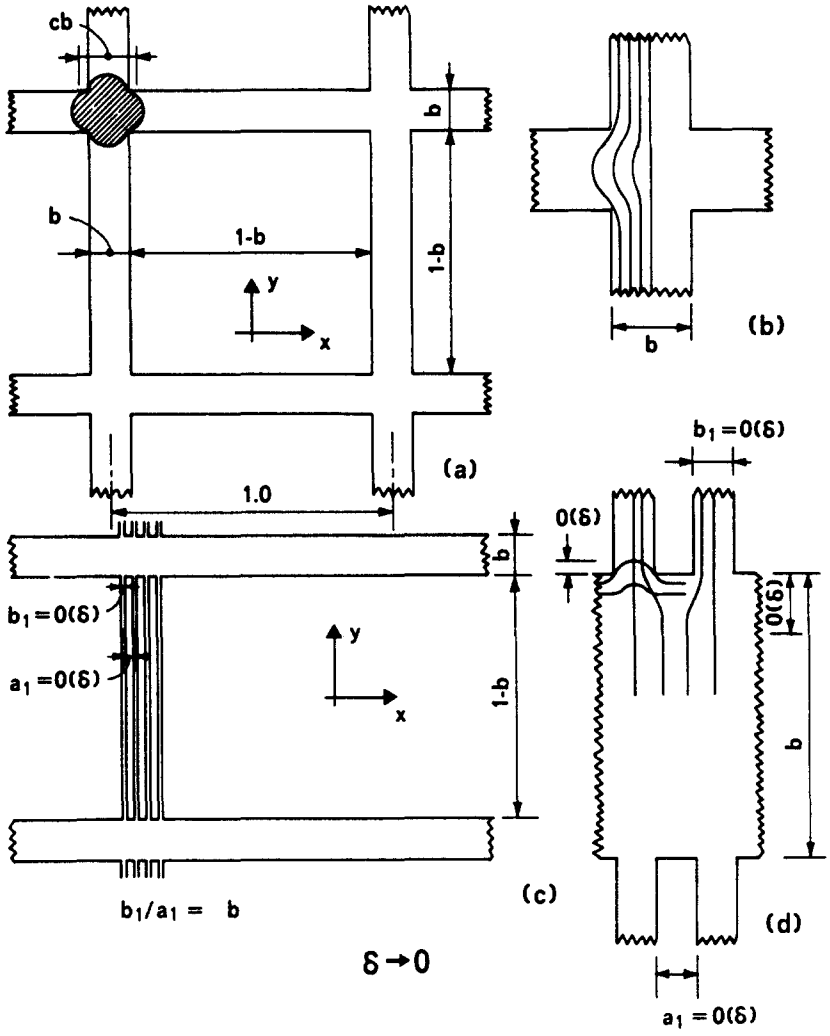

Fig. 2. Intuitive argument showing the higher efficiency of first/second-order microstructures over first/first-order microstructures at low rib densities.

denoted by M_x and M_y and the corresponding equivalent stiffnesses by S_x and S_y. The current derivation is also valid for *plane stress problems* if M_x and M_y are replaced by principal forces (per unit width), N_x and N_y. The normalized *equivalent* stiffnesses are given by

$$\frac{M_i}{S_i} = \frac{M_i(1-b)}{b} + \frac{M_i b}{cb} = M_i \frac{c(1-b)+b}{cb} \qquad (i = x, y) \tag{2}$$

since here we are dealing with a member with two prismatic segments having the respective lengths of $(1-b)$ and b and widths of b and cb. It is assumed that the normalized stiffness of each prismatic segment equals the width of that segment. The *equivalent stiffness* S_i is given by the stiffness of a single prismatic rib whose length equals the combined length (1.0) of the two prismatic segments considered above and whose total change of slope (M_i/S_i) is the same as the sum of the changes of slope over the same two prismatic segments. Since in this case both stiffnesses are the same, the average stiffness S_{AV} becomes

$$S_{AV}^{\wedge} = S_i = \frac{bc}{c(1-b)+b} = \frac{b}{1-b(1-1/c)}. \tag{3}$$

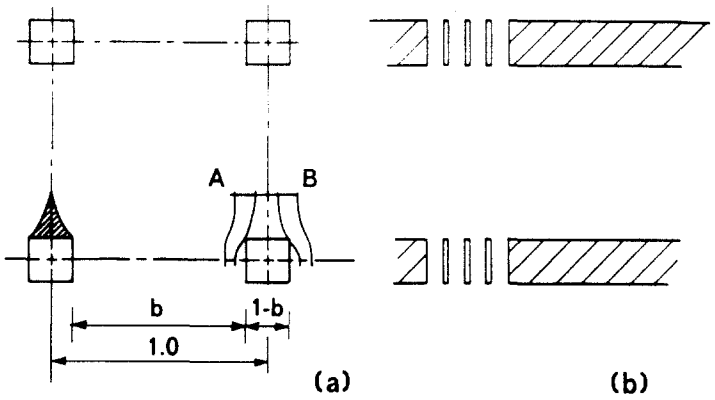

Fig. 3. Intuitive argument showing the higher efficiency of first/first-order microstructures at high rib densities.

For the first/second-order system in Fig. 2(c) the equivalent stiffnesses become

$$\left.\begin{aligned} \frac{M_x}{S_x} &= \frac{M_x(1.0)}{b}, \qquad S_x = b \\ \frac{M_y}{S_y} &= M_y\left(\frac{1-b}{b} + \frac{b}{1}\right) = M_y\frac{1-b+b^2}{b}, \qquad S_y = \frac{b}{1-b+b^2} \end{aligned}\right\} \tag{4}$$

implying

$$S^{\mathrm{B}}_{\mathrm{AV}} = \frac{1}{2}\left(b + \frac{b}{1-b+b^2}\right) = b\frac{1-b/2+b^2/2}{1-b+b^2}. \tag{5}$$

The first/second-order system is more economical if $S^{\mathrm{A}}_{\mathrm{AV}} < S^{\mathrm{B}}_{\mathrm{AV}}$ implying

$$1-b+b^2 < \left(1-\frac{b}{2}+\frac{b^2}{2}\right)\left[1-b\left(1-\frac{1}{c}\right)\right] \tag{6}$$

or

$$0.5 < \frac{1}{c} - \frac{b}{2c} - \frac{b^2}{2}\left(1-\frac{1}{c}\right). \tag{7}$$

Inequality (7) clearly holds if c is significantly less than 2 and b is small. Considering the values of $c = 1.5$, $b = 0.2$, e.g. eqns (3) and (5) imply

$$S^{\mathrm{A}}_{\mathrm{AV}} = \frac{3}{14} = 0.2142857; \qquad S^{\mathrm{B}}_{\mathrm{AV}} = 0.2190476$$

indicating a higher economy for the first/second-order microstructure. However, the same economy does not follow from inequality (7) for high values of b. Moreover, the stress pattern shown in Fig. 2(a) is not valid for high rib-density (b) values approaching unity as can be seen from Fig. 3(a). If the openings (holes) in the plate are small ($(1-b) \times (1-b)$) in comparison to the rib width (b) then by Saint Venant's principle again a uniform stress is achieved at a small distance from the openings (see AB in Fig. 3(a)). This means that only a small part of the system (shaded area in Fig. 3(a)) is *not* stressed in two directions. Replacing the above microstructure with a first/second-order one (Fig. 3(b)) would *increase*

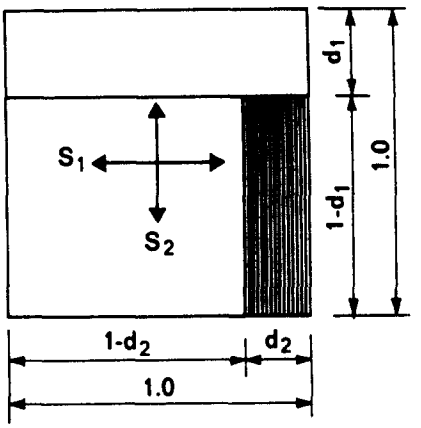

Fig. 4. Rib density values for the calculation of stiffnesses and the specific cost of a first/second-order microstructure.

the areas in one-way stress (shaded areas in Fig. 3(b)) thereby reducing the efficiency of the system.

It appears, therefore, that a first/second-order microstructure is only economical for *low density* perforated plates (having a low "b" value). This conclusion will be confirmed by detailed numerical analysis in a future paper. However, for the purpose of the present investigation, it will be assumed that the solution consists of (i) regions without perforations, and (ii) regions containing first/second-order microstructures.

5. DERIVATION OF THE SPECIFIC COST FUNCTION FOR FIRST/SECOND-ORDER MICROSTRUCTURES

Figure 4 indicates a first/second-order microstructure in which the spacing of the first-order ribs is assumed to be unity (instead of first-order infinitesimal) and the second-order ribs are lumped together over a width d_2 (in reality they are uniformly distributed). Using the method explained in Section 4, the normalized equivalent stiffnesses can be calculated for zero Poisson's ratio ($\nu = 0$) as follows:

$$S_1 = d_1$$

$$\frac{M_2}{S_2} = M_2\left(\frac{1-d_1}{d_2} + \frac{d_1}{1}\right) = \frac{M_2(1-d_1+d_1d_2)}{d_2} \tag{8}$$

$$S_2 = \frac{d_2}{1-d_1+d_1d_2}.$$

It follows that

$$d_2 = \frac{S_2(1-S_1)}{1-S_1S_2} \tag{9}$$

and the specific cost function, ψ, representing the plate area per unit area of the middle surface, then becomes

$$\psi = d_1 + d_2(1-d_1) = S_1 + \frac{S_2(1-S_1)^2}{1-S_1S_2} = \frac{S_1 - 2S_1S_2 + S_2}{1-S_1S_2}. \tag{10}$$

The restrictions on the stiffness values are

$$0 \leqslant S_i \leqslant 1 \qquad (i = 1,2). \tag{11}$$

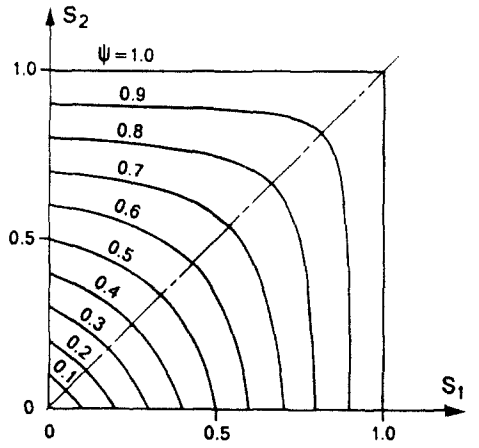

Fig. 5. Specific cost contours for first/second-order microstructures.

The above specific cost function is represented graphically by contour lines on Fig. 5. For $S_1 \to 0$, $S_2 \to 0$, the specific cost function reduces to

$$\psi = S_1 + S_2 \tag{12}$$

which is the correct cost function for Michell structures (in plane stress)[21] and grillages (in flexure)[2, 3] optimized for given compliance. This means that *the present theory reduces to the classical theory of minimum weight trusses and grillages for very low rib densities.*

The derivatives of the above specific cost function are given by

$$\frac{\partial \psi}{\partial S_i} = \frac{(1 - S_j)^2}{(1 - S_i S_j)^2} \qquad \begin{matrix} (i = 1, 2) \\ (j = 2, 1) \end{matrix} \tag{13}$$

Finally, for $S_1 = S_2 = S$, eqns (10) and (13) reduce to

$$\psi = \frac{2S}{1 + S}, \qquad \frac{\partial \psi}{\partial S_i} = \frac{1}{(1 + S)^2} \qquad (i = 1, 2) \tag{14}$$

and for $S_2 = 0$ eqn (10) reduces to

$$\psi = S_1, \qquad \frac{\partial \psi}{\partial S_1} = 1, \qquad \frac{\partial \psi}{\partial S_2} = (1 - S_1)^2. \tag{15}$$

The total "cost" to be minimized is the plate area (without perforations) times the plate thickness h (= const.)

$$\Phi = h \int_D \psi \, dx \, dy. \tag{16}$$

6. VOLUMES OF INTUITIVE DESIGNS FOR SIMPLY SUPPORTED CIRCULAR PLATES

A variational formulation for deriving the absolute minimum plate volume will be discussed in the last few sections of this paper, but to establish useful comparisons with the optimal solution, we first consider a series of intuitive designs for simply supported circular plates with a uniform distributed load.

Using the notation: $\bar{r}$ = radial coordinate, $\bar{M}_\theta$ = circumferential moment (per unit

width), $\bar{M}_r$ = radial moment, $\bar{R}$ = plate radius, $\bar{p}$ = const. = loading per unit area, $\bar{S}_\theta$ = circumferential stiffness (per unit width), $\bar{S}_r$ = radial stiffness (per unit width), $\bar{C}$ = prescribed total compliance, $\bar{\Phi}$ = total plate volume, $\bar{h}$ = plate depth, $\bar{E}$ = Young's modulus, $\bar{w}$ = plate deflection, we introduce the non-dimensional parameters

$$\left.\begin{aligned} r &= \bar{r}/\bar{R}, \qquad M_i = \bar{M}_i/\bar{p}\bar{R}^2 \qquad (i = \theta, r), \\ S_i &= 12\bar{S}_i/E\bar{h}^3, \qquad C = \bar{C}\bar{h}^3E/24\pi\bar{R}^6\bar{p}^2, \\ \Phi &= \bar{\Phi}/2\bar{h}\bar{R}^2\pi, \qquad w = \bar{w}\bar{h}^3\bar{E}/12\bar{R}^4\bar{p}. \end{aligned}\right\} \tag{17}$$

The usual equilibrium condition then becomes

$$(rM_r)'' - M_\theta' = -r, \qquad M_\theta(0) = M_r(0), \qquad M_r(1) = 0 \tag{18a}$$

which may be readily integrated

$$(rM_r)' - M_\theta = -r^2/2, \qquad M_r(1) = 0. \tag{18b}$$

The compliance condition takes the form

$$\int_0^1 [(M_r^2/S_r) + (M_\theta^2/S_\theta)]r\,dr = C = \int_0^1 wr\,dr \tag{19}$$

and the non-dimensional total cost is furnished by

$$\Phi = \int_0^1 \psi(S_\theta, S_r)r\,dr \tag{20}$$

where ψ is given by eqn (10). In the following, the quantity $C\phi$ is used to ensure that the latter takes on a finite value for the limiting case $(1/C) \to 0$.

With the notation described above the intuitive designs can be characterized by:

6.1. *Design A ($M_r \equiv 0$, $S_\theta = M_\theta/k$ where k is a given constant)*

This design consists of circumferential ribs only. Although the external load cannot be transmitted to the supports without radial ribs, this layout can be regarded as a limiting case of a system consisting of both radial and circumferential ribs in which both the radial stiffnesses and radial moments approach zero (or are at least negligibly small). Design A provides a *useful basis for weight comparison* but it is unrealistic for practical purposes because its radial ribs would be subject to very high shear stresses and shear strains. Moreover, the present formulation neglects the effect of shear on the total compliance. Considering plates with a small depth/span ratio, this assumption is realistic for all other designs (which have finite radial stiffness) but not for Design A. By eqns (18a) and (19)

$$M_\theta = r^2/2, \qquad S_\theta = r^2/2k, \qquad k/8 = C \tag{21}$$

so the total cost for Design A is given by $C\Phi = 1/64$.

6.1.1. *Limit of validity.* As $S_\theta \leqslant 1$ also for $r = 1$, Design A is only possible when $1/2k \leqslant 1$, i.e. for

$$1/C \leqslant 16. \tag{22}$$

6.2. *Design B* ($M_r \equiv M_\theta$, $S_i = M_i/k$ $(i = \theta, r)$)

This design consists of a two-way system of ribs throughout. The constant k is to be determined from the magnitude of the prescribed compliance. By eqns (18b) with $M_r \equiv M_\theta$ we have $(rM_r)' - M_r = rM_r' = -r^2/2$ and hence as $M_r(1) = 0$

$$M_r = M_\theta = (1 - r^2)/4, \qquad S_r = S_\theta = S = (1 - r^2)/4k. \tag{23}$$

The compliance constraint (19) gives the value of k

$$2k\int_0^1 [(1 - r^2)r/4]\,\mathrm{d}r = k/8 = C, \qquad k = 8C \tag{24}$$

and the total cost of Design B is thus given by

$$C\Phi = 2C\int_0^1 \frac{(1 - r^2)r\,\mathrm{d}r}{4k + (1 - r^2)} = 32C^2[\ln(32C) - \ln(32C + 1)] + C. \tag{25}$$

In order to obtain the limit of $C\Phi$ for $(1/C) \to 0$ we perform a MacLaurin expansion of $C\Phi$ around $(1/C) = 0$. From this

$$C\Phi = \frac{1}{64} - \frac{1}{3072C} + \frac{1}{131072C^2} \mp \ldots \tag{26}$$

so for $(1/C) \to 0$, Design B gives the same cost as Design A. Variation of $C\Phi$ as a function of C is shown in Fig. 6 in which vertical line segments show the limit of validity of a design.

6.2.1. *Limit of validity.* The constraint $S_\theta \leqslant 1$ should also hold for $r = 0$, so eqns (23) and (24) give that for Design B, C must satisfy

$$1/C \leqslant 32. \tag{27}$$

6.3. *Design C* ($M_\theta \equiv M_r$ *for* $r < g$, $M_\theta \equiv 0$ *for* $r > g$, *and* $S_i = M_i/k$ *throughout the plate* $(i = \theta, r)$)

This design consists of a two-way system of ribs in the inner region $0 \leqslant r < g$ and of radial ribs only in the outer region $g < r < 1$.

With $M_\theta = 0$ for $r > g$, eqns (18b) furnish

$$M_r = (1 - r^3)/6r, \quad \text{for } r > g. \tag{28}$$

Due to continuity of M_r at $r = g$ we have $M_r(g) = (1 - g^3)/6g$, and this is then the boundary condition for the region $0 \leqslant r < g$. Solving eqns (18b), we have

$$M_r = M_\theta = \left(\frac{2}{3g} + \frac{g^2}{3} - r^2\right)\Big/4 \quad \text{for } r < g. \tag{29}$$

Moreover, by eqns (28) and (29), the compliance constraint becomes

$$2k\int_0^g\left(\frac{2}{3g}+\frac{g^2}{3}-r^2\right)(r/4)\,dr + k\int_g^1 [(1-r^3)/6]\,dr$$

$$= (k/6)(g - g^4/4 + 3/4 - g + g^4/4) = k/8 = C, \qquad k = 8C \tag{30}$$

which determines the constant k. The total cost for Design C can then be expressed as

$$\Phi = \int_0^g \frac{2M_r}{8C + M_r} r\,dr + \int_g^1 (M_r/8C) r\,dr$$

$$= g^2 + 32C \ln\{[8C + (1-g^3)/6g]/[8C + (2+g^3)/12g]\}$$

$$+ (1/192C)(3 - 4g + g^4). \tag{31}$$

Note that for $g = 0$ eqn (31) reduces to the total cost value for Design A, and for $g = 1$ furnishes the cost value for Design B.

Moreover, it can be shown by expansion that for $(1/C) \to 0$, eqn (31) gives $C\Phi = 1/64$ which is the total cost for Design A. This result is again to be expected on the basis of the grillage theory[2; 3; 22, pp. 184–188] which indicates that for all fields with $M_\theta \geqslant 0$, $M_r \geqslant 0$, $S_i = M_i/k$ the total volume $C\Phi$ of circular simply supported grillages is an invariant.

6.3.1. *Limits of validity.* Using that $S_i = M_i/k$ should be less than one for $r = 0$, eqns (29) and (30) furnish that for Design C we should have

$$(2/3g + g^2/3)/32C \leqslant 1. \tag{32}$$

6.3.2. *Optimal boundary radius "g".* The usual stationarity condition $d\Phi/dg = 0$ applied to eqn (35) furnishes the optimal value of g

$$\frac{d\Phi}{dg} = 2g - \frac{32C(1+2g^3)}{48Cg^2 + g - g^4} + \frac{64C(1-g^3)}{96Cg^2 + 2g + g^4} + (g^3 - 1)/48C = 0. \tag{33}$$

Variation of $C\Phi_{opt}$ and g_{opt} for Design C is shown in Figs 6 and 7. It can be easily checked that inequality (32), combined with eqn (33) is satisfied for low values of $(1/C)$. The upper limit of validity of Design C is given by inequality (32) and eqn (33)

$$1/C \leqslant 29.4722520. \tag{34}$$

For $(1/C) > 29.4722520$, we can still have a C-type design but the latter is governed by (32) as an equality and *not* by eqn (33). Optimal values of $C\Phi$ and g for this version of Design C are also shown in Figs 6 and 7. The absolute upper limit of Design C is given by (32) as an equality with $g = 1$, furnishing $(1/C) = 32$. At that compliance value, Designs B and C are identical.

Note: It can be seen from Fig. 7 that g_{opt} changes rapidly in the vicinity of $1/C = 0$. As the left-hand side of eqn (33) has limiting value zero for $(1/C) \to 0$, all g-values give the same cost $C\Phi$ for $1/C = 0$ which agrees with the relevant implications of the grillage theory[22]. However, it can be shown that the left-hand side of eqn (33) multiplied by C^2 gives a limiting value of $g_{opt} = 0$ at $(1/C) \to 0$.

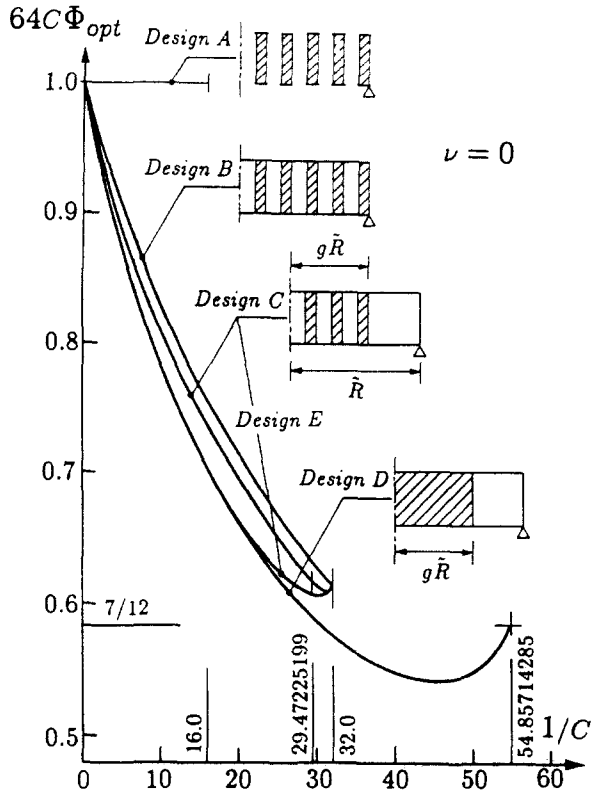

Fig. 6. Comparison of the total weight of optimal solutions (D) with those of various intuitive designs (A, B, C and E) for uniformly loaded simply supported circular plates.

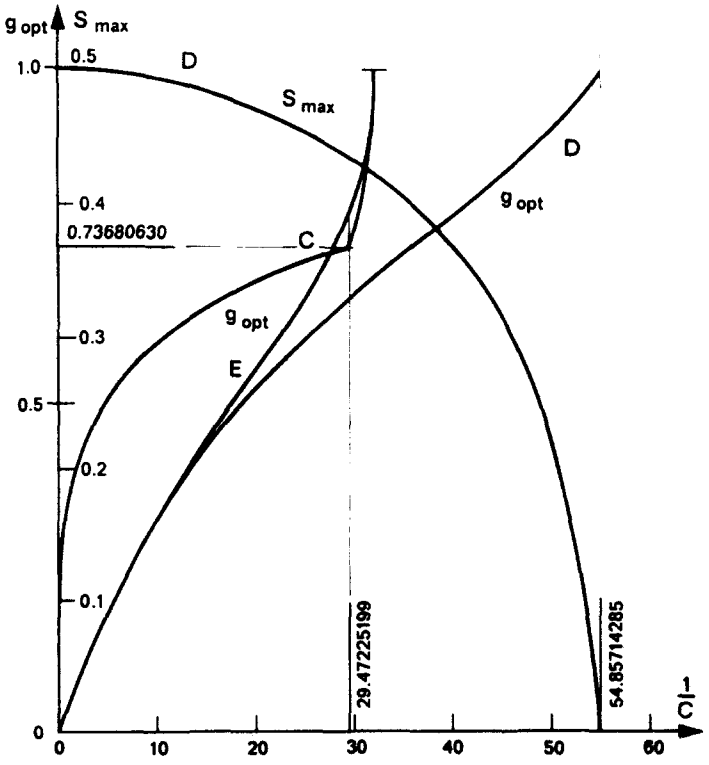

Fig. 7. Optimal values of the maximum stiffness and region boundary radius for uniformly loaded simply supported circular plates.

6.4. *Design D* ($S_\theta = S_r = 1$ *for* $r < g$ *and* $M_\theta = 0$, $S_r = M_r/k$ *for* $r > g$)

This design consists of a solid plate in the inner region ($r < g$) and radial ribs in the outer region ($r > g$). With $M_\theta = 0$ in the region ($r > g$), eqns (18b) give

$$M_r = (1 - r^3)/6r \quad \text{for } r > g. \tag{35}$$

In the inner region ($r < g$), $M_r = -S_r w'' = -w''$ and $M_\theta = -S_\theta w'/r = -w'/r$, where w is the plate deflection. Substituting these expressions into eqns (18b), a compact form can be rewritten

$$[(rw')'/r]' = r/2 \tag{36}$$

such that two integrations yield

$$w' = -Ar + r^3/16 + B/r \tag{37}$$

where A is a constant of integration and the symmetry condition $w'(0) = 0$ implies $B = 0$. M_r is thus given by $M_r = A - 3r^2/16$ in the inner region, and by eqn (35) in the outer region. Continuity of M_r at $r = g$ then gives us

$$A = (1 + g^3/8)/6g. \tag{38}$$

Hence, the moments in the inner region ($r < g$) become

$$\begin{aligned} M_r &= -w'' = A - 3r^2/16 \\ M_\theta &= -w'/r = A - r^2/16 \end{aligned} \quad \text{for } r < g \tag{39}$$

where A is given by eqn (38).

Using these expressions in the compliance constraint we get

$$\begin{aligned} C &= \int_0^g (M_r^2 + M_\theta^2) r\,dr + \int_g^1 kM_r r\,dr \\ &= \int_0^g [(A - 3r^2/16)^2 + (A - r^2/16)^2] r\,dr + \int_g^1 k[(1 - r^3)/6]\,dr \\ &= \frac{1}{36} - \frac{g^3}{72} + \frac{5g^6}{1152} + \frac{k(3 - 4g + g^4)}{24}. \end{aligned} \tag{40}$$

Moreover, the cost is given by

$$\Phi = \int_0^g r\,dr + \int_g^1 [(1 - r^3)/6k] r\,dr = g^2/2 + (3 - 4g + g^4)/24k. \tag{41}$$

Eliminating k from eqn (40) and employing the result in eqn (41), the total volume becomes

$$\Phi = g^2/2 + \frac{(3 - 4g + g^4)^2}{24^2(C - 1/36 + g^3/72 - 5g^6/1152)} \tag{42}$$

Introducing the notation $D = C - 1/36 + g^3/72 - 5g^6/1152$, $B = 3 - 4g + g^4$, the stationarity condition $d\Phi/dg = 0$ for eqn (42) furnishes

$$576gD^2 - 8(1 - g^3)BD - B^2(g^2/24 - 5g^5/192) = 0 \tag{43}$$

which gives g_{opt} for chosen values of C. Also, we get that the following relations hold true at the optimum

$$\left.\begin{aligned} D &= B[(1-g^3)+\sqrt{((1-g^3)^2+3g(g^2/2-5g^5/16))}]/144g \\ &= B(8-5g^3)/576g \\ C &= D+1/36-g^3/72+5g^6/1152, \qquad k=24D/B=(8-5g^3)/24g. \end{aligned}\right\} \tag{44}$$

The optimal cost and boundary radius values ($C\Phi_{opt}$ and g_{opt}) are shown in Figs 6 and 7. The g and k values given by eqns (43) and (44) for given C values must satisfy the constraint $S_r \leqslant 1$ at $r = g$ where $S_r = M_r/k$ takes on its maximum value in the outer region. This implies that $(1-g^3)/6gk = 4(1-g^3)/(8-5g^3) \leqslant 1$, which is clearly fulfilled for all admissible g values ($0 \leqslant g \leqslant 1$).

The upper limiting value of $(1/C)$ for Design D can be calculated from eqn (40) with $g = 1$ as the entire feasible plate volume in this case is filled with material and hence no design can furnish a greater feasible $(1/C)$. The limiting value is thus

$$1/C = 54.85714286. \tag{45}$$

6.5. *Design E ($S_\theta \equiv S_r \equiv M_\theta/k_1 \equiv M_r/k_1$ for $r < g$ and $M_\theta \equiv 0$, $S_r = M_r/\alpha k_1$ for $r > g$ where k_1 and α are constants)*

This design is similar to Design C except that different constants (moment/stiffness ratios) are used for the inner and outer regions.

The moment fields for this design are the same as for Design C and are given by eqns (28) and (29). The compliance constraint (19) then takes the form

$$C = k_1(g/6-g^4/24)+\alpha k_1(1/8-g/6+g^4/24)$$

or

$$k_1 = aC \tag{46}$$

with

$$a = 6/[g-g^4/4+\alpha(3/4-g+g^4/4)]. \tag{47}$$

The total cost for this design is given by

$$\begin{aligned} \Phi &= \int_0^g [2M_r/(k_1+M_r)]r\,dr + \int_0^1 (M_r/\alpha k_1)r\,dr \\ &= g^2 + 4aC\ln\frac{1+(1-g^3)/6gaC}{1+(2+g^3)/12gaC} + (3-4g+g^4)/24aC\alpha. \end{aligned} \tag{48}$$

Expression (48) implies that optimization of Design E is a two-parameter problem, $\min \Phi = \Phi(g,\alpha)$, subject to the constraints $S_r(0) \leqslant 1$ and $S_r(g) \leqslant 1$. On the basis of eqns (28) and (29), these constraints can be rewritten as

$$S_r(0) = (2/3g+g^2/3)/4aC \leqslant 1 \tag{49}$$

$$S_r(g) = (1-g^3)/6gaC\alpha \leqslant 1. \tag{50}$$

Detailed numerical investigations have shown that for $(1/C) > 3$ the optimal solution for Design E is controlled by constraint (49) as an equality. For $(1/C) < 3$ the sensitivity

of Φ for changes in g and α is extremely low and the relevant equations were found somewhat illconditioned. It can be seen from Fig. 6 that the cost (volume) of Design E is higher than that of Design D but the difference is small for $(1/C) < 20$. The optimal cost values at $(1/C) = 10$ were found to be $64C\Phi_D = 0.78550116$ and $64C\Phi_E = 0.78557618$ while at $(1/C) = 5$ they were $64C\Phi_D = 0.87837477$ and $64C\Phi_E = 0.87837626$. For $(1/C) < 3$ the conclusion $\Phi_D < \Phi_E$ could not be confirmed because the difference between the two cost values was beyond the resolving power of the computer. The optimal g-values for Design E are shown in Fig. 7.

CONCLUSIONS

(1) The problem of optimizing the microstructure of perforated elastic continua for a compliance constraint was re-examined in the light of certain fundamental principles of solid mechanics.

(2) Considering perforated plates under either flexure or plane stress, a comparison of two classes of microstructures, having the same prescribed stiffness values in the corresponding principal directions, was presented. It was found that at low rib densities, a system with first- and second-order infinitesimal rib spacings in the two directions is more economical than those with the same order of rib spacing in both directions.

(3) As a consequence of Saint Venant's principle, the proposed micromodel assumes that on their interior ribs of second-order infinitesimal width are subject to stresses in the direction of their middle plane only. Hence these ribs do not contribute to the stiffness in the direction normal to their middle plane. In this respect, the proposed formulation differs from recent mathematical studies[12, 13] of this problem.

(4) On the basis of the above micromodel, a specific cost function for perforated plates in bending or plane stress was derived. The latter gives a relationship between the stiffnesses in the principal directions and the material volume per unit area of the plate middle surface.

(5) The proposed specific cost function was then used for examining the design of circular, uniformly transversely loaded elastic perforated plates of a prescribed compliance.

(6) It was shown earlier by the first author[22, pp. 184–188] that all solutions for simply supported circular *grillages* have the same optimal weight if (a) the principal moments are everywhere positive and (b) the beam stiffnesses are made proportional to the moment values. Considering five intuitively selected designs, the same conclusion has been confirmed for circular perforated plates whose average rib density approaches zero (i.e. whose prescribed compliance approaches infinity).

(7) In Part II of this study a variational analysis is employed in order to find optimal designs for transversely loaded axially symmetric plates, and this analysis shows that first/second-order ribs do not improve economy as compared to use of just first-order ribs.

REFERENCES

1. K.-T. Cheng and N. Olhoff, An investigation concerning optimal design of solid elastic plates. *Int. J. Solids Structures* **16**, 305–323 (1981).
2. W. Prager and G. I. N. Rozvany, Optimal layout of grillages. *14th International Congress of Theoretical and Applied Mechanics*, Delft, August 1976; also *J. Struct. Mech.* **5**, 1–18 (1977).
3. G. I. N. Rozvany, Grillages of maximum strength and maximum stiffness. *Int. J. Mech. Sci.* **14**, 651–666 (1972).
4. K.-T. Cheng, On non-smoothness in optimal design of solid, elastic plates. *Int. J. Solids Structures* **17**, 931–948 (1981).
5. N. Olhoff, K. A. Lurie, A. V. Cherkaev and A. V. Fedorov, Sliding regimes and anisotropy in optimal design of vibrating axisymmetric plates. *Int. J. Solids Structures* **17**, 931–948 (1981).
6. K.-T. Cheng and N. Olhoff, Regularized formulation for optimal design of axisymmetric plates. *Int. J. Solids Structures* **18**, 153–170 (1982).
7. G. I. N. Rozvany, N. Olhoff, K.-T. Cheng and J. Taylor, On the solid plate paradox in structural optimization. *J. Struct. Mech.* **10**, 1–32 (1982).
8. C.-M. Wang, G. I. N. Rozvany and N. Olhoff, Optimal plastic design of axisymmetric solid plates with a maximum thickness constraint. *Comput. Struct.* **18**, 653–665 (1984).
9. R. V. Kohn and M. Vogelius, A new model for thin plates with rapidly varying thickness. *Int. J. Solids Structures* **20**, 333–350 (1984).

10. M. P. Bendsøe, Generalized plate models and optimal design. *Proc. IMA Workshop on "Homogenization and Effective Moduli"*, University of Minnesota, October (1984).
11. R. V. Kohn and G. Strang, Optimal design for torsional rigidity, *Hybrid and Mixed Finite Element Methods* (Edited by S. N. Atluri, R. H. Gallagher and O. C. Zienkiewicz), pp. 281–288. Wiley, New York (1983).
12. K. A. Lurie, A. V. Fedorov and A. V. Cherkaev, Regularization of optimal design problems for bars and plates, Parts I and II. *J. Optimization, Theory Applic.* **37**, 499–521, 523–543 (1982).
13. K. A. Lurie, A. V. Fedorov and A. V. Cherkaev, On the existence of solutions to some problems of optimal design for bars and plates. *J. Optimization Theory Applic.* **42**, 247–281 (1984).
14. K. A. Lurie and A. V. Cherkaev, G-Closure of a set of anisotropically conducting media in the two-dimensional case. *J. Optimization Theory Applic.* **42**, 283–304 (1984).
15. K. A. Lurie and A. V. Cherkaev, Exact estimates of conductivity of composites formed by two isotropically conducting media taken in prescribed proportion. *Proc. R. Soc. Edinb.* **99A**, 71–78 (1984).
16. K. A. Lurie and A. V. Cherkaev, Optimal structural design and relaxed controls. *Optimal Control Applic. Meth.* **4**, 387–392 (1981).
17. R. V. Kohn and G. Strang, Optimal design and relaxation of variational problems, I, II and III. *Commun. Pure Appl. Math.* **XXXIX**, 113–137, 139–181, 353–377 (1986).
18. R. V. Kohn and G. Strang, Structural design optimization, homogenization and relaxation of variational problems, *Lecture Notes in Physics* (Edited by R. Burridge, G. Papanicolau and S. Childress), No. 154. Springer, Berlin (1982).
19. B. de Saint Venant, *Mémoires des Savants Etrangers*, Vol. 14 (1855).
20. S. P. Timoshenko and J. N. Goodier, *Theory of Elasticity*. McGraw-Hill, New York (1951).
21. A. G. M. Michell, The limits of economy of material in frame structures. *Phil. Mag.* Sect. 6 **8**, 589–597 (1904).
22. G. I. N. Rozvany, *Optimal Design of Flexural Systems*. Pergamon Press, Oxford (1976).